East European Journal of Physics. **4.** 213-221 (2022)
DOI:10.26565/2312-4334-2022-4-22 ISSN 2312-4334

DETECTION OF LYSOZYME AMYLOID FIBRILS USING TRIMETHINE CYANINE DYES: SPECTROSCOPIC AND MOLECULAR DOCKING STUDIES[†]

Olga Zhytniakivska[a,*], Uliana Tarabara[a], Atanas Kurutos[b,c], Kateryna Vus[a], Valeriya Trusova[a], Galyna Gorbenko[a]

[a]*Department of Medical Physics and Biomedical Nanotechnologies, V.N. Karazin Kharkiv National University 4 Svobody Sq., Kharkiv, 61022, Ukraine*
[b]*Institute of Organic Chemistry with Centre of Phytochemistry, Bulgarian Academy of Sciences, Acad. G. Bonchev str., bl. 9, 1113, Sofia, Bulgaria*
[c]*Department of Pharmaceutical and Applied Organic Chemistry, Faculty of Chemistry and Pharmacy Sofia University St. Kliment Ohridski, 1 blv. J. Bourchier, Sofia, 1164, Bulgaria*
**Corresponding Author: olga.zhytniakivska@karazin.ua*
Received October 15, 2022; revised November 18, 2022; accepted November 21, 2022

Due to their unique photophysical and photochemical properties and high sensitivity to the beta-pleated motifs, cyanine dyes are increasingly used as molecular probes for the identification and characterization of amyloid fibrils *in vitro* and the visualization of amyloid inclusions *in vivo.* In the present study the spectroscopic and molecular docking techniques have been employed to evaluate the amyloid sensitivity and the mode of interaction between the trimethine cyanine dyes and the native (LzN) and fibrillar (LzF) lysozyme. It was found that the trimethine association with non-fibrilar and fibrillar forms of lysozyme is accompanied by the changes in the dye aggregation extent. The molecular docking studies indicate that: i) the trimethines form the most stable complexes with deep cleft of the native lysozyme; ii) the dye binding to non-fibrillar protein is governed by the hydrophobic interactions, π-stacking contacts between aromatic or cyclopentane ring of the cyanine and Trp in position 63 or 108 and hydrogen bonds between the OH-groups of the trimethines and acceptor atoms of Asp 101 (AK3-7) and Gln 57 (AK3-8) of LzN; iii) cyanine dyes form the energetically most favorable complexes with the groove Gly 2-Leu 4/Ser 8-Trp 10 of the lysozyme fibril core; iv) cyanines-LzF interaction is stabilised by hydrophobic contacts, π-stacking interaction and hydrogen bonds. The dyes AK3-7, AK3-5 and AK3-11 were selected as the most prospective amyloid probes.
Keywords: Trimethine cyanine dyes, lysozyme, amyloid fibrils.
PACS: 87.14.C++c, 87.16.Dg

During the last decades, cyanine dyes have found numerical applications in a variety of research areas including bioanalysis, pharmacology, medicine, optoelectronics, photoelectrochemistry, laser technologies, etc. [1-6]. Likewise, these probes appeared to be especially useful for the detection of the disease-related protein aggregates, amyloid fibrils, due to their advantages such as i) long wavelength absorption and emission maxima [7,8]; ii) dependence of the cyanine photophysical properties on the protein environment resulting from the flexibility of the polymethine chain in their structure [9, 10]; iii) significant enhancement of fluorescence emission upon binding to amyloid fibrils [11-13]; iv) the characteristic fluorescence turn-on mechanism in the presence of aggregated proteins [14,15]; v) the ability to form self-assembled supramolecular complexes [15-17], vi) rather high amyloid sensitivity and specificity of cyanines [10,13,14]. More specifically, cyanine dyes were effectively used for: i) *in vivo* fluorescence imaging of amyloid β-plaques [11,18]; ii) monitoring the fibrillation kinetics of amyloidogenic proteins [12]; iii) preventing and modulating protein fibrillization [16,19], to name only a few.

Recently, we have reported the ability of trimethine cyanine compounds to detect the insulin amyloid fibrils [15]. Briefly, based on the comprehensive analysis of the spectral characteristics of trimethines in the buffer solution and in the presence of control and fibrillar insulin we demonstrated that the dyes under study are capable of distinguishing between the non-aggregated and fibrillar insulin [15]. Moreover, the dye AK3-11 was selected as the most effective amyloid sensor among the studied cyanines due to conversion of the AK3-11 non-emissive assemblies in aqueous solution and non-fibrillized insulin to the highly fluorescent monomeric species in the presence of the fibrillar insulin [15]. Furthermore, we demonstrated that these trimethine derivatives possess the potency to interfere with the insulin aggregation [19]. However, all the above studies were performed using the insulin as a model protein. Besides we didn't evaluate the influence of protein charge and hydrophobicity on the amyloid-sensing potential of the cyanine dyes. To fill this gap, the aim of the present study to investigate the interactions between the trimethine cyanine dyes and the lysozyme amyloid fibrils using the spectroscopic and molecular docking techniques. More specifically, we concentrated our efforts on characterizing both the spectral responses and the potential binding sites of the cyanines in the presence of fibrillar and non-aggregated lysozyme.

MATERIALS AND METHODS

Materials

Egg yolk lysozyme (Lz) was purchased from Sigma, USA. The trimethine cyanine dyes (Figure 1) were synthesized at the University of Sofia, Bulgaria, as described previously [15]. All other reagents were of analytical grade and used without further purification.

[†] ***Cite as***: O. Zhytniakivska, U. Tarabara, A. Kurutos, K. Vus, V. Trusova, and G. Gorbenko, East Eur. J. Phys. **4**, 213 (2022), https://doi.org/10.26565/2312-4334-2022-4-22

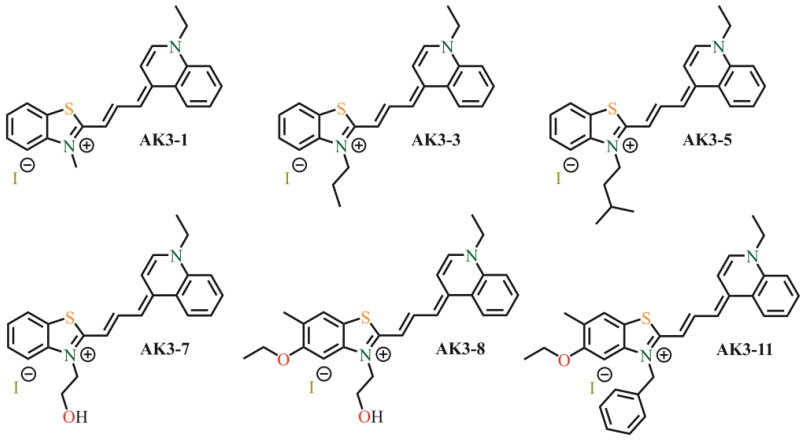

Figure 1. Structural formulas of the trimethine cyanine dyes

Preparation of working solutions

The stock solutions of the examined trimethine cyanine dyes were prepared immediately before measurements by dissolving the dyes in dimethyl sulfoxide. The concentrations of the dyes were determined spectrophotometrically, using their extinction coefficients [15]. The lysozyme stock solution (10 mg/ml) was prepared by dissolving the protein in 10 mM glycine buffer (pH 2.0). This solution was used as reference for non-aggregated protein (LzN). The amyloid fibrils of lysozyme were prepared by the protein incubation in 10 mM glycine buffer at pH 2 and 60°C for 14 days. The amyloid nature of the protein aggregates was confirmed by ThT assay and the transmission electron microscopy. Hereafter, the fibrillar lysozyme is designated as LzF.

Spectroscopic measurements

The steady-state fluorescence spectra were collected on a FL-6500 spectrofluorimeter (Perkin-Elmer Ltd., Beaconsfield, UK) at 20ºC with excitation wavelength 590 nm using the 10 mm path-length quartz cells. The excitation and emission slit widths were set at 10 nm. To record the fluorescence spectra of the cyanines in the dye-protein complexes, the appropriate amounts of the stock solutions of the non-aggregated or fibrillar lysozyme were added to each dye in 5 mM sodium phosphate buffer (pH 7.4).

The absorption spectra of the dyes were acquired on Shimadzu UV-2600 Spectrophotometer (Japan) at 25ºC using 10-mm path-length quartz cuvettes. To measure the absorption spectra of cyanine dyes in the aqueous phase or in the complexes with lysozyme, appropriate amounts of the stock dye solutions in DMSO were added either to 5 mM sodium phosphate buffer (pH 7.4) or directly to the working protein solutions and were incubated for one hour. The deconvolution of the dye absorption spectra was performed in the Origin 9.0 (OriginLab Corporation, Northampton, USA) using the log-normal asymmetric function (LN) [20]:

$$A = A_{\max} \exp\left[-\frac{ln2}{\ln^2(\rho)} \ln^2\left(\frac{a-v}{a-v_c}\right) \right] \tag{1}$$

where A denominates the absorbance, $A_{\max}$ is the maximum absorbance, v is the wavenumber, v_c is the peak position, ρ expresses the asymmetry of the function defined as:

$$\rho = \frac{v_c - v_{\min}}{v_{\max} - v_c} \tag{2}$$

where $v_{\min}$ and $v_{\max}$ represent the wavenumber values at half-absorbance. The parameter a designates the limiting wavenumber:

$$a = v_c + \frac{(v_{\max} - v_{\min}) \cdot \rho}{\rho^2 - 1} \tag{3}$$

Molecular docking studies

To define the most energetically favorable binding sites for the examined dyes on the lysozyme amyloid fibrils, the molecular docking studies were performed using the the AutoDock (version 4.2) incorporated in the PyRx software (version 0.8) [21]. To further characterize the nature of the dye-protein interactions, the protein-ligand interaction profiler PLIP was used [22]. The dye structures were built in MarvinSketch (version 18.10.0) and optimized in Avogadro (version 1.1.0) [23,24].The crystal structures of hen egg white lysozyme (PDB ID: 3A8Z) was taken from the Protein Data Bank. The lysozyme model fibril was built from the K-peptide, GILQINSRW (residues 54–62 of the wild-type protein), using the CreateFibril tool as described previously [25].

RESULTS AND DISCUSSION

Fluorescence spectra of trimethines in the unbound state and in the presence of the native and fibrillar lysozyme are presented in Figure 2.

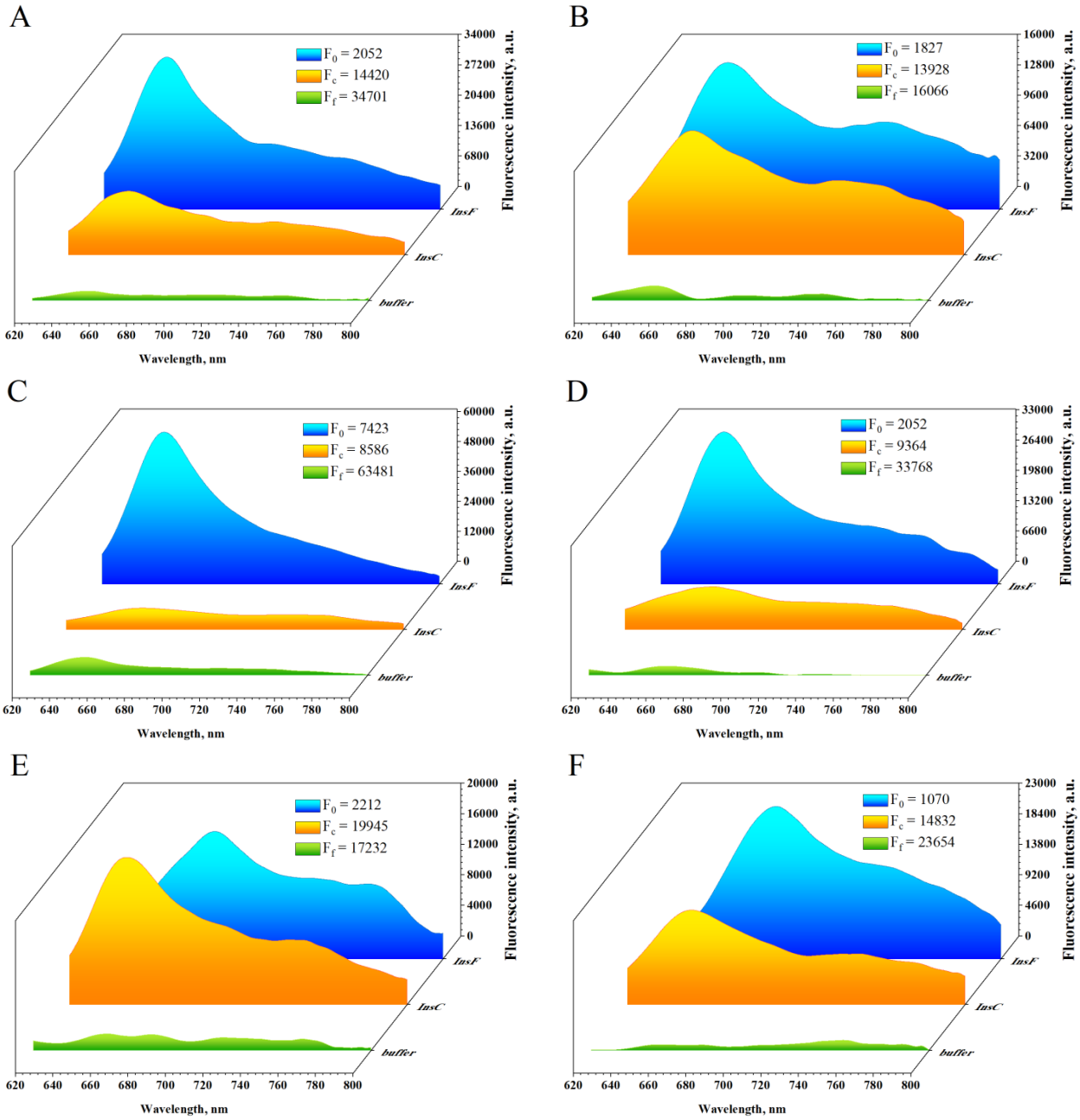

Figure 2. Fluorescence response of trimethine cyanine dyes to the non-fibrillar and fibrillar lysozyme. The dye and protein concentrations were 0.5 μM and 3.4 μM, respectively.

The photophysical properties of the examined cyanines in the buffer solution were examined previously and summarized in the Table 1. Specifically, the trimethines AK3-1, AK3-3, AK3-5 and AK3-7 exhibit a negligible fluorescence in buffer solution with the emission maxima located between 640 and 651 nm, depending on the dye chemical structure [15]. Besides, trimethines AK3-8 and AK3-11 are characterized by a negligible fluorescence intensity in buffer and do not show clear emission and excitation maxima [15]. The addition of the non-fibrillar lysozyme to the AK31, AK33, AK38 and AK3-11 in the buffer solution was accompanied by a significant enhancement of the dye fluorescence intensity along with a slight bathochromic shift (1-6 nm) of the excitation and emission maxima. In turn, the association of AK3-5 and AK3-7 with LzN was followed by a slight fluorescence increase coupled with a ~ 70-nm shift of the dye excitation maxima to the shorter wavelengths. Simultaneously, a ~ 15 nm bathochromic shift of the AK3-5 and AK3-7 emission maxima was observed in the presence of non-fibrillar lysozyme. As shown in Figure 2 and Table 1, the spectral response of the trimethine dyes (except AK3-8) to the fibrillar lysozyme lies in a strong increase of the dye fluorescence (I_f) as opposed to that in buffer (I_0) and in the presence of nonfibrillar protein (I_n), with a magnitude of

the fluorescence intensity increase depending on the dye chemical structure. The fluorescence maxima of the trimethines are shifted by approximately 9-15 nm towards longer wavelengths compared to those observed either in the non-aggregated proteins or in the buffer solution, as illustrated in Table 1.

Table 1. Spectral characteristics of the trimethine cyanine dyes in the presence of native and fibrillar lysozyme

Dye	Free dye			Control protein			Fibrillar protein			
	λ_{ex} (nm)	λ_{em} (nm)	F_0, (a.u.)	λ_{ex} (nm)	λ_{em} (nm)	F_c, (a.u.)	λ_{ex} (nm)	λ_{em} (nm)	F_f, (a.u.)	ADF
AK3-1	627	644	3470	627	653	14420	640	654	34701	5.84
AK3-3	626	646	1827	634	656	13928	637	656	16066	1.17
AK3-5	631	645	7423	559	661	8586	635	653	63481	7.39
AK3-7	628	642	2052	559	661	9364	634	654	33768	11.90
AK3-8	n.d.*	651	2212	625	650	19945	668	676	17232	-1.22
AK3-11	n.d.*	658	1070	630	656	14832	668	677	23654	8.24

λ_{ex} – maximum of the excitation spectra; λ_{em} –maximum of the emission spectra; n.d.[a] – not determined because of negligible fluorescence intensity; I_0, I_n, and I_f – fluorescence intensity of the dyes in buffer and in the presence of control and fibrillar proteins, respectively

By analogy with the insulin model protein, we determine the specificity of the examined trimethines also to the lysozyme amyloid fibrils. Therefore, we calculated the amyloid detection factor (ADF) (Table 1) characterizing the ability of a dye to selectively detect the fibrillar state over its native structure relative to the background fluorescence of the dye in buffer [15, 26]:

$$ADF = \frac{I_f - I_n}{I_0}. \quad (4)$$

It appeared that the trimethines under study (except AK3-8) are characterized by the positive ADF values in the presence of the fibrillar lysozyme, being indicative of their higher sensitivity to the fibrillar protein aggregates compared to the non-aggregated state. Although the enchanced fluorescence was observed for AK3-8 in the presence of LzF, the magnitude of fluorescence intensity increase was higher in the presence of monomeric lysozyme, as judged from the negative amyloid detection factor for this dye. In the presence of lysozyme fibrils the amyloid specificity was found to decrease in the row AK3-7 → AK3-11→ AK3-5 → AK3-1 → AK3-3→ AK3-8. It appeared that AK3-7, possessing the lowest sensitivity to the insulin amyloid fibrils [15], has demonstrated the largest ADF value in the presence of the lysozyme amyloid fibrils. The relatively high amyloid detection factors were observed in the presence of lysozyme for AK3-11 and AK3-5 dyes. Remarkably, these dyes were highly sensitive also to the insulin amyloid fibrils [15]. However, the ADF values of the trimethines were found to be significantly higher in the presence of insulin amyloid fibrils (ADF values exceeded 15 for all cyanines except AK3-7 in the presence of insulin fibrils [15]) compared to lysozyme, suggesting a sensitivity of the examined cyanines to the fibril morphology.

To interpret the observed fluorescence responses and the binding data of the cyanine dyes, in the following studies we analyzed their absorption spectra free in buffer solution as well as in the presence of control and fibrillar protein (Figure 3). For a more detailed analysis (by analogy with the data obtained for the insulin fibrils), we performed the decomposition of these absorption spectra using the log-normal asymmetric function (Eq. 1) [20].

The absorption spectra of AK3-5 and AK3-3 in buffer solution were represented as a sum of two separate bands, with a short-wavelength and long-wavelength spectral components corresponding to the dimeric and monomeric dye species, respectively. The corresponding absorption spectra of AK3-1, AK3-7, AK3-8 and AK3-11 in aqueous phase were deconvoluted into three bands representing the dye monomers, dimers and higher order aggregates (Figure 4). The deconvolution of the absorption spectra allowed us to calculate a set of parameters, viz.: i) the amplitude $A_{\max}$ (Table 2): i) the peak position ν_c, related to the environmental polarity [20] (Table 3); ii) the full width at half-maximum of the band (FWHM) (Table 4); and iii) the peak asymmetry parameter ρ (Table 5).

Table 2. The amplitude of the bands in the absorption spectra of cyanines

	Band	AK3-1	AK3-3	AK3-5	AK3-7	AK3-8	AK3-11
buffer	I	40000	97000	50000	84168	20739	15353
solution	II	8500	35171	33680	39000	8816	9711
	III	14000	-	-	8000	27500	18934
LzN	I	43112	22100	70503	50720	27768	14355
	II	11652	9935	52474	52102	24562	5360
	III	7895	11434	-	2224	9627	30784
LzF	I	52327	32383	74203	46437	44261	53443
	II	13891	6468	60928	54887	25834	22866
	III	4918	1757	-	39	2091	7296

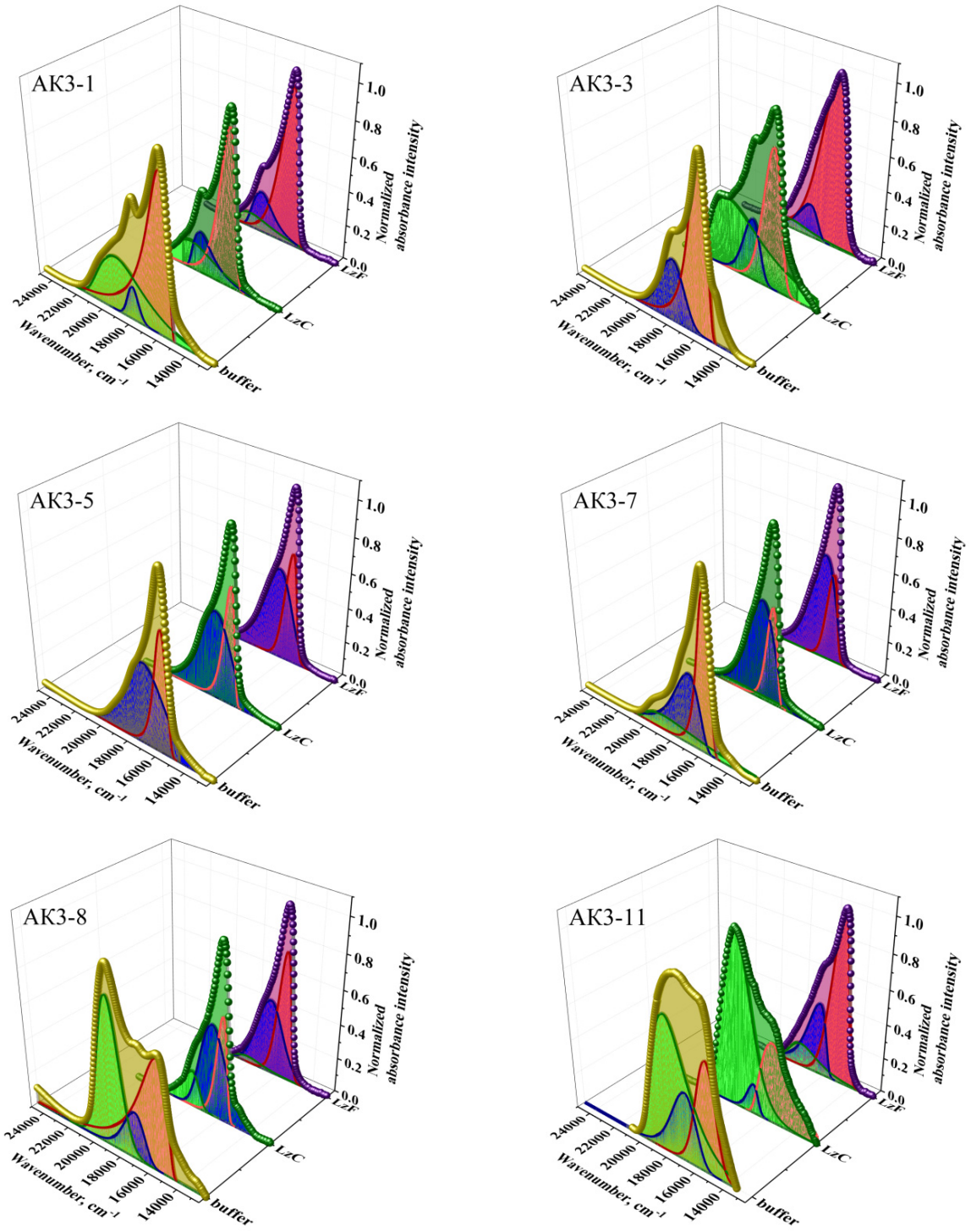

Figure 3. Deconvolution of trimethines absorption spectra in buffer solution and in the presence of the non-fibrillar and fibrillar lysozyme. Band I is marked red, band II – blue, band III – green.

The incubation of AK3-1, AK3-5 та AK3-8 (Table 2) with the non-fibrillar lysozyme resulted in the following changes of the amplitude of the bands in comparison with those observed in the buffer solution: i) the rise in the amplitude of the bands I (a 1.1-fold, 1.4-fold and 1.3-fold increase) and II (a 1.4-fold, 1.6-fold and 2.8-fold increase); ii) the drop of the amplitude of the band III for AK3-1 (1.8 times) та AK3-8 (2.9 times) and the band narrowing; iii) a 3.3-fold, 1.7-fold and 1.1-fold decrease in the amplitude of the band I for AK3-3, AK3-7 and AK3-11, respectively; iv) the rise in the amplitude of the bands II (AK3-7) and band III (AK3-11). It should be noted that the absorption spectra of AK3-3 in the non-fibrillar lysozyme were deconvoluted into three separate bands, where for the short- (dimeric dye form) and long-wavelength (monomeric dyes form) bands the 3.5-fold and 4.4-fold drop of the amplitude was observed. Likewise, the incubation of AK3-3 with the non-fibrillar lysozyme resulted in the appearance of the III short-wavelength band of H-aggregates, the intensity of which even exceeded the amplitude of the band II.

Table 3. The position of the band (ν_c , cm^{-1}) in the buffer solution and in the presence of non-fibrillar and fibrillar lysozyme

Dye	Band	buffer solution	LzN	LzF
AK3-1	I	16007	16024	15924
	II	18100	18056	17943
	III	19300	18780	18764
AK3-3	I	15900	15608	15516
	II	17900	17025	17115
	III	-	18858	18434
AK3-5	I	15900	15858	15778
	II	17200	16930	16692
AK3-7	I	15900	15888	15854
	II	17000	16636	16494
	III	19000	18921	19000
AK3-8	I	15700	15871	15681
	II	17300	16622	16717
	III	19100	18041	18302
AK3-11	I	15550	15691	15100
	II	17000	16934	16500
	III	18300	18289	17800

Furthermore, while comparing the ν_c values (Table 3), it can be seen that monomeric lysozyme produced a hypsochromic shift of the monomer band I (AK3-3), dimer band II (all dyes except AK3-1), and the H-aggregates band III (AK3-1, AK3-7 and AK3-8). In turn, the position of the band I for AK3-8 та AK3-11 shifted to the higher wavenumbers. Moreover, the incubation of AK3-1, AK3-5 та AK3-8 with the LzN resulted in the increase of the asymmetry parameter (Table 5) and the full width at half-maximum (Table 4) of the band II (AK3-1 and AK3-7). In the meantime, the presence of the non-fibrillar lysozyme led to the decrease of the full width at half-maximum of the band I (Table 4). Taken together, we can conclude that the trimethine dyes AK3-1, AK3 5, AK3-7 and AK3-8 bind to the native lysozyme mainly in the form of monomers and dimers, while AK3-3 and AK3-11 show a tendency to aggregate in the presence of the non-fibrillar lysozyme.

The deconvolution of the absorption spectra of the trimethine dyes demonstrated that the dominating dye species in the presence of the lysozyme fibrils are the dye monomers and dimers. More specifically, the incubation of AK3-1, AK3-5, AK3-8 та AK3-11 with the fibrillar protein resulted in a 1.3, 1.8, 2.1 and 3.5-fold increase of the relative integral intensities of the band I along with 1.6, 1.5, 2.9 and 2.4-fold enhancement of the amplitude of the band II, respectively (Table 2). This effect was accompanied by the drop of the amplitude of the band III for AK3-1 (2.8 times), AK3-8 (13 times) та AK3-11 (2.6 times) (Table 2). At the same time, it can be seen that the lysozyme fibrils produced a significant attenuation in FWHM of the band I (AK3-1, AK3-5, AK3-8 та AK3-11) and band II (AK3-5, AK3-11), whereas in the case of AK3-1 and AK3-8 this parameter showed a slight increase for the bands II (AK3-1, AK3-8) and III (AK3-8) (Table 4).

Table 4 The full width at half-maximum of the band (FWHM, cm-1) in the buffer solution and in the presence of non-fibrillar and fibrillar lysozyme

Dye	Band	Buffer solution	LzC	LzF
AK3-1	I	1767	1314	1405
	II	910	1647	1747
	III	3795	3378	2931
AK3-3	I	1422	1436	2077
	II	2000	1383	1623
	III	-	4544	2183
AK3-5	I	1000	891	979
	II	3251	2696	2471
AK3-7	I	1000	862	883
	II	2159	2243	2185
	III	4803	10385	3448
AK3-8	I	2347	863	1052
	II	1750	2138	2181
	III	1832	1461	2054
AK3-11	I	1582	2256	1353
	II	2027	922	1568
	III	2935	2475	2356

This effect was accompanied by the lowered ν_c values of the bands I and II for AK3-1, AK3-5 and AK3-11 presumably arising from the reduced environmental polarity of the dye monomers and dimers associated with the fibrillar lysozyme (Table 3). On the contrary, the insulin fibrils did not exert influence on the position of the band III for AK3-1, AK3-8 and AK3-11. Remarkably, the higher amplitude increase of he band I for AK3-5 and AK3-11 indicates that the

binding of monomers is more favorable for these dyes. The complexation of AK3-3 with the fibrillar lysozyme, similar to the non-aggregated protein, led to the rise of the relative contribution of the bands III and II to the overall spectrum (Table 2). Besides, the relative integral intensities of the bands II and III were 1.5 and 6.5 times lower than those observed in the presence of the non-aggregated lysozyme. Moreover, the incubation of AK3-3 with the lysozyme fibrils resulted in a 1.5-fold increase of the monomer band. This effect was accompanied by the lowered ν_c values of the band I. Taken together, the above findings indicate that AK3-3 binds to the lysozyme amyloid fibrils presumably in the form of monomers. The incubation of AK3-7 with the fibrillar lysozyme resulted in the significant drop of the amplitude of the bands II and III in comparison with those observed in the buffer and control protein. The band III corresponding to the dye H-aggregates was almost indistinguishable. Furthermore, the enhancement of the amplitude of the band I along with the lowered ν_c values of the band I indicate that bound monomers are the dominating dye species in the presence of the lysozyme fibrils.

Table 4. The asymmetry of the function (ρ , cm^{-1})) in the buffer solution and in the presence of non-fibrillar and fibrillar lysozyme

Dye	Band	Buffer solution	LzC	LzF
AK3-1	I	0.42	0.62	0.66
	II	1.02	1.82	1.56
	III	1.53	1.48	1.73
AK3-3	I	0.54	0.81	1.00
	II	0.81	0.81	0.66
	III	-	2.00	2.30
AK3-5	I	0.67	0.66	0.88
	II	1.05	0.91	0.85
AK3-7	I	0.67	0.75	0.85
	II	0.59	1.21	1.27
	III	2.66	4.84	3.95
AK3-8	I	0.45	0.72	0.84
	II	0.75	1.20	1.03
	III	1.00	0.70	1.35
AK3-11	I	0.91	1.69	0.83
	II	0.76	0.77	0.61
	III	1.54	1.21	1.59

At the next step of the study the molecular docking technique was used to identify the trimethine-lysozyme binding sites. As represented in Figure 4, the trimethines tend to form the most stable complexes with deep cleft of the native lysozyme.

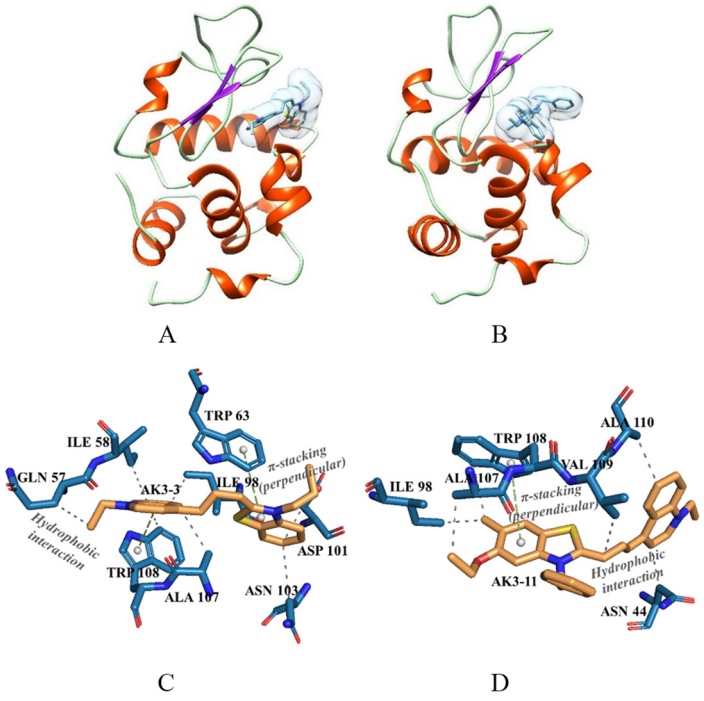

Figure 4. Most favorable modes of interactions between AK3-3 (A, C), AK3-11 (B, D) and native lysozyme obtained using the AutoDock (panels A, B) and PLIP (panels C and D). The grey dashed lines and green dashed line on the panels C and D represent the hydrophobic interactions and π-stacking contacts between the dye molecule and the lysozyme residues, respectively.

The free energy of cyanine – LzN binding was found to follow the order: AK3-11 (-8.18 kcal/mol) > AK3-1 (-7.90 kcal/mol) > AK3-3 (-7.78 kcal/mol) > AK3-7 (-7.42 kcal/mol) > AK3-5 (-7.34 kcal/mol) > AK3-8 (-7.01 kcal/mol). As judged from the PLIP analysis, the hydrophobic interactions play a significant role in the binding of cyanines to the non-aggregated lysozyme and involve Asn 44 (only AK3-11), Gln 57 (except AK3-5, AK3-11), Ile 58 (except AK3-8, AK3-11), Asn 59 (AK3-1), Trp 62 (AK3-5), Trp 63 (AK3-5, AK3-7, AK3-8), Leu 75 (AK3-5), Ile 98 (except AK3-8), Asp 101 (except AK3-7, AK3-11), Asn 103 (except AK3-8, AK3-11), Ala 107 (except AK3-7, AK3-8), Trp 108 (except AK3-7, AK3-8), Val 109 (AK3-8, AK3-11) and Ala 110 (AK3-11). Moreover, the trimethines were found to form π-stacking contacts between aromatic or cyclopentane ring of the cyanine and Trp in position 63 (in the case of AK3-1, AK3-3, AK3-5) and 108 (except AK3-7, AK3-8). The AK3-7, AK3-8 complexes with the native lysozyme are additionally stabilized by hydrogen bonds between the OH-groups of the trimethines and acceptor atoms of Asp 101 (AK3-7) and Gln 57 (AK3-8) of LzN.

Figure 5 represents the energetically most favorable cyanine complexes with the groove Gly 2-Leu 4/Ser 8-Trp 10 of the lysozyme fibril core, which are stabilised by hydrobhobic contacts with Leu 4, Trp 10 as well as π-stacking interactions between cyanine dyes and the side chains of the groove residues (Figure 5, panel B). In addition, the complexes of AK3-7 and AK3-8 with LzF are stabilized by hydrogen bonds involving Ile 3 (AK3-7, AK3-8) and Arg 9 (AK3-8). The binding energies appeared to be comparable with the native lysozyme and follow the order: AK3-11 (-7.78 kcal/mol) > AK3-3 (-7.11 kcal/mol) > AK3-1 (-6.74 kcal/mol) > AK3-5 (-6.59 kcal/mol) > AK3-7 (-6.43 kcal/mol) > AK3-8 (-6.13 kcal/mol).

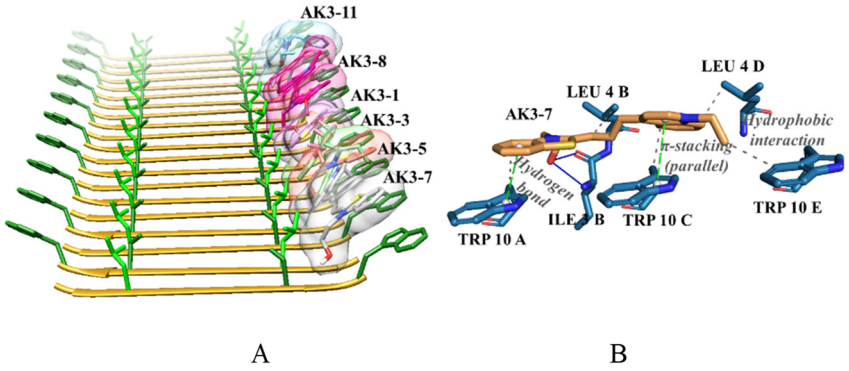

Figure 5. The complexes of trimethine dyes with the fibrillar lysozyme obtained using the AutoDock (A). Representative interactions between AK3-11 and groove Gly 2-Leu 4 / Ser 8-Trp 10 of the lysozyme fibril revealed by PLIP (B). The grey dashed lines on the panel B represent the hydrophobic interactions between the dye molecule and the groove, while the green dashed line and blue solid line display the π-stacking contacts and hydrogen bonds, respectively.

CONCLUSIONS

To summarize, in the present study the optical spectroscopy and molecular docking techniques were used to investigate the interactions between the trimethine cyanine dyes and lysozyme in the non-fibrillar and amyloid states. It was found that all cyanines under study are capable of distinguishing between the non-aggregated and fibrillar protein forms. The dyes AK3-7, AK3-5 and AK3-11 appeared to possess the highest amyloid sensitivity due to: i) significant fluorescence enhancement in the presence of LzF produced by the binding of the dye monomers to fibrillar lysozyme; ii) the lower binding affinity of the dye monomers to the nonfibrillar lysozyme in comparison with the aggregated protein. In turn, significantly lower ADF values observed for AK3-3, AK3-1 and AK3-8 were interpreted as arising from the binding of dye monomers to the nonfibrillar lysozyme. The fluorescence response of cyanines in the presence of lysozyme fibrils led us to conclude that the trimethine dyes under study are sensitive to the fibril morphology.

Acknowledgements

This work was supported by the Ministry of Education and Science of Ukraine (the Young Scientist projects No0120U101064 “Novel nanomaterials based on the lyophilic self-assembled systems: theoretical prediction, experimental investigation and biomedical applications” and the project “Development of novel means of medical diagnostics by biomedical nnanotechnologies and modern ultrasonic and fluorescence methods”).

ORCID IDs

Olga Zhytniakivska, https://orcid.org/0000-0002-2068-5823; **Uliana Tarabara,** https://orcid.org/0000-0002-7677-0779
Atanas Kurutos, https://orcid.org/0000-0002-6847-198X; **Kateryna Vus,** https://orcid.org/0000-0003-4738-4016
Valeriya Trusova, https://orcid.org/0000-0002-7087-071X; **Galyna Gorbenko,** https://orcid.org/0000-0002-0954-5053

REFERENCES

[1] P. Pronkin, and A. Tatikolov, Molecules, **27**(19), 6367 (2022). https://doi.org/10.3390/molecules27196367
[2] M. Bokan, G. Gellerman, and L. Patsenker. Dyes Pigm. **171**, 107703 (2019). https://doi.org/10.1016/j.dyepig.2019.107703
[3] M. Guo, P. Diao, Y.-J. Ren, F. Meng, H. Tian, and S.-M. Cai, Sol. Energy Mater. Sol. Cells, **88**, 33 (2005). https://doi.org/10.1016/j.solmat.2004.10.003

[4] C. Shi, J.B. Wu, and D. Pan. J. Biomed. Opt. **21**(5), 05901 (2022). https://doi.org/10.1117/1.JBO.21.5.050901
[5] G.D. Pelle, A.D. Lopez, and M.S. Fiol, Int. J. Mol. Sci. **22**(13), 6914, (2021). https://doi.org/10.3390/ijms22136914
[6] O. Cavuslar, and H. Unal, RSC Advances, **5**, 22380 (2015). https://doi.org/10.1039/C5RA00236B
[7] H.L. Yang, S.Q. Fang, Y.W. Tang, et al., Eur. J. Med. Chem. **179**, 736 (2019). http://dx.doi.org/10.1016/j.ejmech.2019.07.005
[8] X. Mu, F. Wu, R. Wang, Z. Huang, et al., Sens Actuators B. Chemical. **338**, 29842 (2021). https://doi.org/10.1016/j.snb.2021.129842
[9] K.D. Volkova, V.B. Kovalska, O.A. Balanda, R.J. Vermeij, V. Subramaniam, Y.L. Slominskii, and S.M. Yarmoluk, J. Biochem. Biophys. Methods, **70,** 727, (2007). https://doi.org/10.1016/j.jbbm.2007.03.008
[10] V.B. Kovalska, M.Yu. Losytskyy, O.I. Tolmachev, et al., J. Fluoresc. **22,** 1441 (2012). https://doi.org/10.1007/s10895-012-1081-x
[11] J. Yan, J. Zhu, K. Zhou, et al., Chem. Commun. **53,** 1441 (2017). https://doi.org/10.1039/C7CC05056A
[12] T. Smidlehner, H. Bonnet, S. Chierici, and I. Piantanida, Bioorg. Chem. **104,** 104196 (2020). https://doi.org/10.1016/j.bioorg.2020.104196
[13] R. Sabate, and J. Estelrich, Biopolymers, **72**(6), 455 (2003). https://doi.org/10.1002/bip.10485
[14] G.Q. Gao, A.W. Xu, RSC Adv. **3,** 21092 (2013). https://doi.org/10.1039/C3RA43259A
[15] O. Zhytniakivska, A. Kurutos, U. Tarabara, K. Vus, V. Trusova, G. Gorbenko, N. Gadjev, and T. Deligeorgiev, J. Mol. Liq. **311**, 113287 (2020), https://doi.org/10.1016/j.molliq.2020.113287
[16] S. Chernii, Y. Gerasymchuk, M. Losytskyy, D. Szymanski, et al., PLOS One, **16**(1), e0243904 (2021). https://doi.org/10.1371/journal.pone.0243904
[17] K. Vus, U. Tarabara, A. Kurutos, O Ryzhova, G. Gorbenko, et al., Mol. Biosyst. **13**(5), 1970 (2017). https://doi.org/10.1039/c7mb00185a
[18] H.L. Yang, S.Q. Fang, Y.W. Tang, et al. Eur. J. Med. Chem, **179**, 736 (2019). https://doi.org/10.1016/j.ejmech.2019.07.005
[19] K. Vus, M. Girych, V. Trusova, et al. J. Mol. Liq. **276,** 541 (2019). https://doi.org/10.1016/j.molliq.2018.11.149
[20] M. Bacalum, B. Zorila, and M. Radu, Anal. Biochem. **440,** 123 (2013). https:// doi.org/10.1016/j.ab.2013.05.031
[21] S. Dallakyan, and A.J. Olson, Methods Mol. Biol. **1263**, 243 (2015). https://doi.org/10.1007/978-1-4939-2269-7_19
[22] S. Salentin, S. Schreiber, V.J. Haupt, M.F. Adasme, and M. Schroeder, Nucleic Acids Res. **43**, W443 (2015), https://doi.org/10.1093/nar/gkv315.
[23] P. Csizmadia, in: *Proceedings of ECSOC-3, the third international electronic conference on synthetic organic chemistry*, edited by E. Pombo-Villar, R. Neier, and S.-K. Lin (MDPI, Basel, Switzerland, 1999), pp. 367-369. https://doi.org/10.3390/ECSOC-3-01775
[24] M.D. Hanwell, D.E. Curtis, D.C. Lonie, T. Vandermeersch, E. Zurek, and G.R. Hutchison, J. Cheminform. **4**, 17 (2012), https://doi.org/10.1186/1758-2946-4-17
[25] V. Trusova, East Eur. J. Phys. **2,** 51 (2015), https://periodicals.karazin.ua/eejp/article/view/4010/3568
[26] P.L. Donabedian, M. Evanoff, F.A. Monge, D.G. Whitten, and E.Y. Chi, ACS Omega, **2**, 3192 (2017). https://doi.org/10.1021/acsomega.7b00231

ДЕТЕКТУВАННЯ АМІЛОЇДНИХ ФІБРИЛ ЛІЗОЦИМУ ЗА ДОПОМОГОЮ ТРИМЕТИНЦІАНІНОВИХ БАРВНИКІВ: СПЕКТРОСКОПІЧНІ ДОСЛІДЖЕННЯ ТА МОЛЕКУЛЯРНИЙ ДОКІНГ

Ольга Житняківська[a], Уляна Тарабара[a], Анатас Курутос[b,c], Катерина Вус[a] , Валерія Трусова[a], Галина Горбенко[a]
[a]Кафедра медичної фізики та біомедичних нанотехнологій, Харківський національний університет імені В.Н. Каразіна м. Свободи 4, Харків, 61022, Україна
[b]Інститут органічної хімії та фітохімії Академії Наук Болгарії, Вул. Акад. Бончева, 9, 1113, Софія, Болгарія;
[c]Кафедра фармацевтичної та прикладної органічної хімії, Факультет хімії та фармації, Софійський університет імені Св. Климента Охридського, 1164, Софія, Болгарія;

Завдяки своїм унікальним фотофізичним і фотохімічним властивостям, а також їх високій чутливості до бета-складчастих мотивів, ціанінові барвники широко застосовуються як молекулярні зонди для ідентифікації та характеризації амілоїдних фібрил in vitro та візуалізації амілоїдних включень in vivo. В даній роботі, за допомогою спектроскопічних методів та молекулярного докінгу досліджено амілоїдну специфічність та механізми взаємодії між триметинціаніновими барвниками та нативним (LzN) і фібрилярним (LzF) лізоцимом. Встановлено, що асоціація триметину з нефібрилярним і фібрилярним білком супроводжується зміною ступеня агрегації барвників. Дослідження молекулярного докінгу між триметиновими барвниками та лізоцимом у нативному та амілоїдному станах показують, що: i) триметини мають тенденцію утворювати найбільш стабільні комплекси з «deep cleft» нативного лізоциму; ii) зв'язування барвника з нефібрилярним білком регулюється гідрофобними взаємодіями, π-стекінгом між ароматичним або циклопентановим кільцем ціаніну та Trp у положенні 63 або 108 та водневими зв'язками між OH-групами триметинів і акцепторними атомами Asp 101 (AK3-7) і Gln 57 (AK3-8); iii) ціанінові барвники утворюють енергетично найбільш сприятливі комплекси з борозенкою Gly 2-Leu 4/Ser 8-Trp 10 ядра фібрили лізоциму; iv) взаємодія ціаніни-LzF стабілізується гідрофобними контактами, π-стекінговою взаємодією та водневими зв'язками. Барвники AK3-7, AK3-5 та AK3-11 були обрані як найбільш перспективні амілоїдні зонди.

Ключові слова: Триметинові ціанінові зонди, лізоцим, амілоїдні фібрили